

Superfluid ^3He Confined to a Single $0.6 \mu\text{m}$ Slab Stability and Properties of the A-like Phase Near the Weak Coupling Limit

R. G. Bennett · L. V. Levitin · A. Casey ·
B. Cowan · J. Parpia · J. Saunders

Received: date / Accepted: date

Abstract We present the first study of the phase diagram of a thick film of superfluid ^3He confined within a nanofabricated slab geometry. This cryogenic microfluidic chamber provides a well-defined environment for the superfluid, in which both the regular geometry and surface roughness may be fully characterised. The chamber is designed with a slab thickness $d = 0.6 \mu\text{m}$ and 3 mm thick walls to allow pressure tuning of the effective confinement between 0 and 5.5 bar. Over this range the zero temperature superfluid coherence length, ξ_0 , decreases by approximately a factor of two from 77 to 40 nm. Samples have so far been cooled to 350 μK . We use nuclear magnetic resonance (NMR) to ‘finger-print’ the superfluid order parameter, with the static field applied perpendicular to the slab. To enable us to resolve high quality NMR signals from the tiny amount of superfluid ^3He in the slab, we have developed a spectrometer using a two stage SQUID amplifier with unprecedented sensitivity. Simple NMR Zeugmatography allows the slab signal to be unambiguously distinguished from that of a small bulk liquid region near the fill line. The measured slab transition temperature, T_c^{slab} , shows a suppression proportional to ξ_0^2 , as expected theoretically, but the absolute suppression is less than expected. Below T_c^{slab} , an A-like phase is stable over a significant temperature range. A transition temperature, T_{AX} , is measured on warming from a so far unidentified phase, occurring at lower temperatures, into the A-phase. At the pressures investigated (3 to 5.5 bar) the transition appears to occur at an approximately fixed value of the effective confinement $d/\xi(T_{AX})$. In this geometry we predict that the A-phase will be stable to $T = 0$ at zero pressure.

Keywords superfluid · Helium-3 · confinement · slab · NMR · phase transition

PACS 67.30.H- · 67.30.ht · 67.30.er

R. G. Bennett · L. V. Levitin · A. Casey · B. Cowan · J. Saunders
Dept. of Physics, Royal Holloway, University of London, Egham, Surrey, TW20 0EX, UK
Tel.: +44-(0)1784-434455
Fax: +44-(0)1784-437520
E-mail: j.saunders@rhul.ac.uk

J. Parpia
LASSP and CCMR, Cornell University, Ithaca, NY 14853 USA

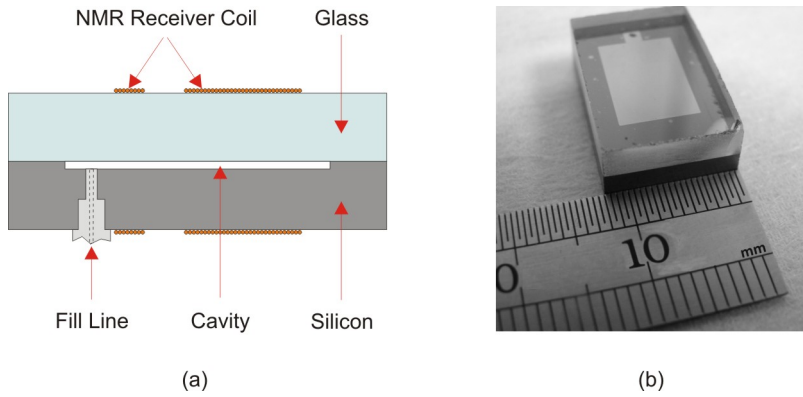


Fig. 1 (Color online) (a) Schematic diagram of the cell. The depth of the helium cavity has been enlarged for clarity. (b) Photograph of the bonded cell, prior to attaching the fill line. The helium cavity can clearly be seen in the centre.

1 Introduction

At a diffusively scattering wall, all components of the superfluid order parameter are suppressed and they recover over a length scale on the order of the temperature dependent coherence length, $\xi(T)$, away from the wall [1]. In the Ginzburg-Landau regime $\xi(T)$ is given by,

$$\xi(T) = \sqrt{7\zeta(3)/20}\xi_0 \left(1 - T/T_c^{\text{bulk}}\right)^{-1/2}, \quad (1)$$

where $\zeta(3)$ is the Riemann zeta function, T_c^{bulk} is the bulk superfluid transition temperature and

$$\xi_0 = \hbar v_F / (2\pi k_B T_c), \quad (2)$$

is the zero temperature coherence length, which can be thought of as the ‘size’ of a Cooper pair. ξ_0 is a function of pressure and varies from 77 nm at zero pressure to about 15 nm at melting pressure.

Numerous authors [2–6] have considered superfluid ^3He confined to a thin slab and the influence of confinement on the phase diagram. In the weak coupling limit, most closely approached at $p = 0$ for superfluid ^3He , it is found that either the A-phase or the planar phase¹ is stable down to $T = 0$ below a critical slab thickness of between about 700 and 350 nm. For thicker slabs the stable phase should be a distorted B-phase. In this work we have studied a $d = 0.6 \mu\text{m}$ thick slab of ^3He at pressures between 0 and 5.5 bar and down to a temperature of 350 μK .

2 Experimental Details

Previous experiments [7–9] have confined ^3He between stacks of 1000–400 thin Mylar or polyethylene sheets, separated by tiny microspheres. Our cell, shown schematically in Fig. 1(a), consists of a single 635nm deep, 10 mm \times 7 mm rectangular cavity, nanofabricated into a 3 mm thick, 17.5 mm \times 12 mm piece of silicon. The cavity depth was

¹ These two phases are degenerate in the weak coupling limit.

measured using a profilometer. A matching piece of 3 mm thick Hoya SD2 glass [10] was then anodically bonded over the top to seal the cavity. The wall thickness was chosen to avoid distortion of the cavity under pressure.

Prior to the bonding of the glass, a stepped hole for the fill line was ultrasonically drilled through the silicon. The fill line was epoxied in, using stycast 2850FT, after the anodic bonding and there exists a small ‘dead volume’ around the end of the fill line in which some bulk ^3He collects. The signal from the ^3He in this volume (Sect. 3) provides a useful internal measure of T_c^{bulk} .

Our experimental probe is nuclear magnetic resonance (NMR), which provides the most effective means of characterising the superfluid order parameter. We use pulsed NMR, with the static field applied perpendicular to the plane of the slab. The low number of spins ($< 10^{18}$) and very small filling factor ($\sim 4 \times 10^{-5}$) of our sample require a highly sensitive NMR spectrometer in order to resolve the weak signal. To meet this need we developed a pulsed NMR spectrometer [11], based around a two-stage SQUID amplifier. The SQUID has a coupled energy sensitivity as low as $20 h$ and the spectrometer has a noise temperature of 5 mK at 1 MHz.

The ^3He inside the cell is cooled by a $\sim 2.5 \text{ m}^2$ silver sinter heat exchanger, in close proximity to the cell. Thermometry is provided by a ^{195}Pt NMR thermometer, calibrated against a ^3He melting curve thermometer.

3 Results

We begin with a description of the signal in the normal state. Fig. 2(a) displays a typical normal state signal at a pressure of 0 bar. The signal was qualitatively the same at all pressures. Two signals are present, separated by about 600 Hz. By applying magnetic field gradients we could carry out simple NMR zeugmatography (described below) from which we could unambiguously identify the sharp signal as coming from ^3He in the slab and the broader signal as coming from the ^3He in the dead volume.²

The effect of applying a gradient parallel to the plane of the slab is shown by the bold (blue online) signal in Fig. 2(b). The slab signal is broadened and flattened out, consistent with it coming from a large area, such as the slab. The bulk signal is relatively unchanged and just moves to a higher frequency, consistent with it coming from a small, localised region, such as the dead volume. The effect of applying a gradient perpendicular to the slab is also consistent with this hypothesis, as shown by the thin (red online) signal in Fig. 2(b). The bulk signal actually becomes somewhat sharper in this case and we therefore maintain a field gradient perpendicular to the slab during our measurements.

We now discuss our observations in the superfluid state; all data discussed in this section were taken on warming. In the superfluid state, at all pressures, both signals exhibited temperature dependent frequency shifts as shown in Fig. 3 for $p = 0.75\text{bar}$. The slab signal had a negative frequency shift, consistent with that of the dipole-unlocked A-phase ($\mathbf{d} \perp \mathbf{l}$) [12], as expected for our cell geometry and field orientation. The bulk signal had a positive frequency shift, much larger in magnitude than the slab frequency shift, consistent with the that of the B-phase at a wall parallel to an applied magnetic field.

² From this point onwards we shall refer to the signals as the ‘slab signal’ and ‘bulk signal’.

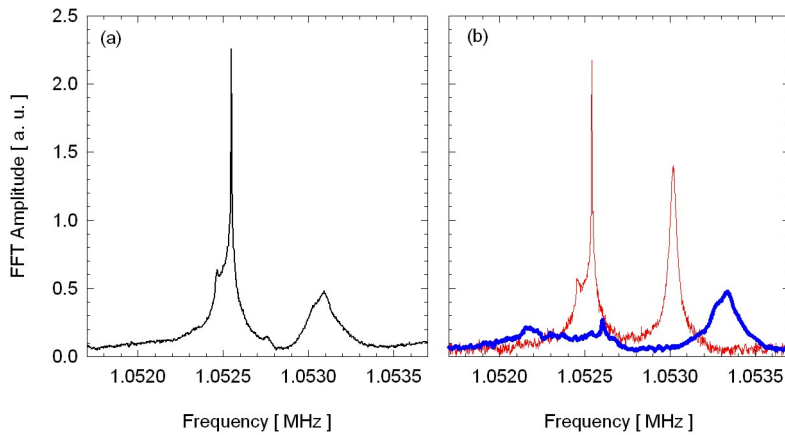


Fig. 2 (Color online) (a) The signal in the normal state at 0 bar in absence of any field gradients. The slab signal is on the left and the bulk signal is on the right. (b) The effect of field gradients. The bold (blue) line shows the effect of a 3 mT/m gradient applied parallel to the plane of the slab. The thin (red) line shows the effect of a 4 mT/m gradient applied perpendicular to the slab. See text for further discussion.

It can also be seen from Fig. 3 that the superfluid transition temperature of the slab, T_c^{slab} , is suppressed compared to T_c^{bulk} . Kjälman, Kurkijärvi and Rainer [13] calculated the transition temperature of a slab of ^3He between two diffusively scattering walls. For slabs thicker than about $d = 8\xi_0$ they found their numerical calculation to be in good agreement with the Ginzburg-Landau result,

$$T_c^{\text{slab}}/T_c^{\text{bulk}} = \exp(-\pi^2\xi(0)^2/d^2) \approx 1 - \pi^2\xi(0)^2/d^2, \quad (3)$$

where $\xi(0)^2 = (7\zeta(3)/20)\xi_0^2$ (Eq. 1). The suppression that we observe is proportional to $\xi(0)^2$, but its magnitude is less than predicted by Eq. 3. We attribute this to partial specularly of the cell walls, since there should be no suppression of T_c^{slab} for specular walls [13]. The partial specularity could be related to the low surface roughness of the silicon and glass ($\sim 0.2\text{nm}$). The effect of introducing a surface layer of ^4He will be explored in future experiments.

For $p > 3$ bar we have observed a phase transition from a so far unidentified low temperature phase into the A-phase. The nature of the low temperature phase and the transition will be described elsewhere in these proceedings [14]. The reduced thickness at the transition $d/\xi(T_{AX})$, where $\xi(T)$ is given by Eq. 1 and T_{AX} is the transition temperature observed on warming, has only a weak, linear dependence on pressure. In Fig. 4 we show our measured values of T_{AX} at several pressures on the bulk phase diagram [15]. Clearly the domain of the A-phase has been greatly increased. The lines through our data points are generated from a fit to $d/\xi(T_{AX})$ as a function of pressure. The dash-dot line is a result of using the Ginzburg-Landau temperature dependence of $\xi(T)$ from Eq. 1. This line reaches $T = 0$ at a non-zero critical pressure, $p_c = 0.66$ bar, below which only the A-phase should be stable in our cell. At this pressure $\xi_0 = 69$ nm, corresponding to $d/\xi_0 = 9.2$. Therefore, at $p = 0$ bar we would expect the A-phase to be stable down to $T = 0$ for d less than a critical thickness of $d_c = 9.2 \times 77$ nm = 708 nm, in reasonable agreement with the upper limit of the theoretical predictions.

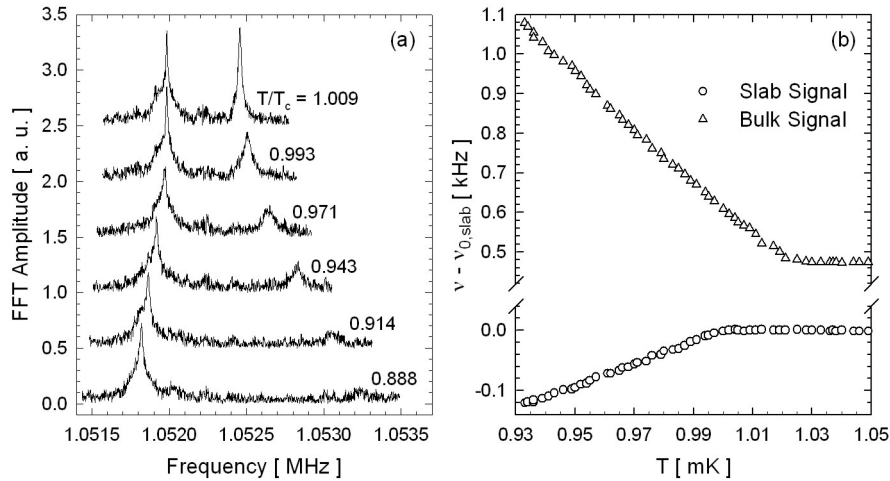


Fig. 3 (a) Evolution of the slab and bulk signals as a function of reduced temperature, close to T_c^{bulk} , at $p = 0.75$ bar. The increased noise on these signals compared to those of Fig. 2 is a result of us using less averaging for these signals since their frequency is shifting as the cell warms up. (b) Frequency shifts of the slab and bulk signals, relative to the slab Larmor frequency, $\nu_{0,\text{slab}}$, as a function of temperature near T_c^{bulk} . All data taken on warming.

However, for $p = 2.18$ bar (not shown on Fig. 4) we observed only the A-phase down to a temperature of $350 \mu\text{K}$; significantly below T_{AX} as predicted by the Ginzburg-Landau line in Fig. 4. One possible explanation could be suppression of the transition on cooling [14]. Alternatively this result could be related to the temperature dependence of the coherence length. The Ginzburg-Landau temperature dependence is expected to only be valid near T_c^{bulk} . A potentially more accurate expression for $\xi(T)$ at lower temperatures, which results in the dashed line in Fig. 4, is

$$\xi(T) = \hbar v_F / (\pi \Delta(T)), \quad (4)$$

where $\Delta(T)$ is obtained using the interpolation formula for the gap function as given by Einzel [16]. Using this form of $\xi(T)$ we obtain a higher critical pressure of 2.47 bar, which would explain why we do not observe a transition for $p = 2.18$ bar.

4 Conclusions

We have established that it is possible to effectively cool a thin slab of ^3He , confined inside a regular, well characterized, nano-fabricated geometry, into the superfluid state. Good quality NMR signals were observed using SQUID based NMR techniques developed in our laboratory. The A-phase is stabilised at low pressures close to the weak coupling limit, and the conditions for its stability to $T = 0$ established. Details of the pressure dependence of the A-phase frequency shift, an analysis of the suppression of the gap by confinement from that data, and an examination of the consistency with the observed suppression of T_c^{slab} , will be reported elsewhere. The walls of the present cell appear to be partially specular and an attempt to demonstrate full specularly by ^4He preplating will be the subject of future work. This is also required for future experiments in more confined geometries, where elimination of T_c suppression is important.

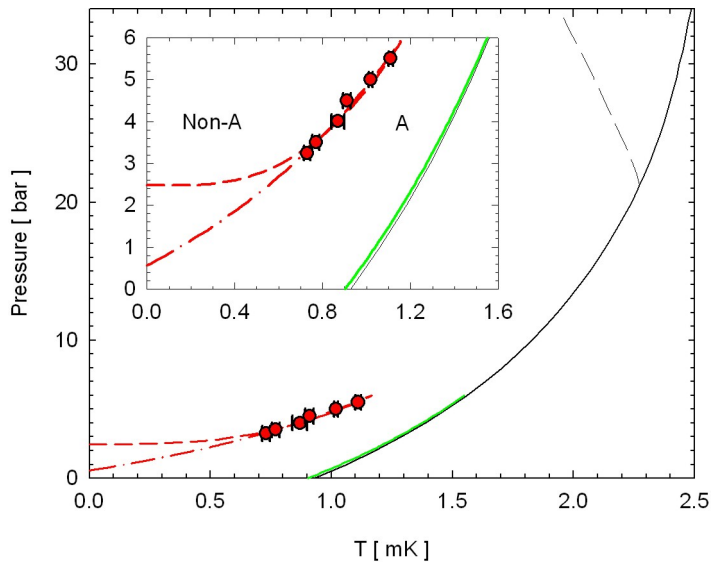


Fig. 4 (Color online) Comparison of our data to the bulk phase diagram. The thin solid and dashed lines represent T_c and T_{AB} for bulk liquid respectively [15]. The filled (red) circles are our measurements of T_{AX} . The bold dashed (red) line represents our fit to T_{AX} using the Ginzburg-Landau temperature dependence for $\xi(T)$, and the bold dash-dot (red) line from using $\xi(T)$ as given by Eq. 4. The bold solid (green) line represents a fit to our values of T_c^{slab} . The inset shows a close-up of the region for $p \leq 6$ bar.

This will open the possibility to study quasi-2D superfluid ^3He , where confinement gives rise to size quantization of the normal state and where new order parameters are expected.

Acknowledgements We would like to acknowledge the contributions of Svetoslav Dimov and Robert Ilic in fabricating the cell. Work at Royal Holloway was supported by the EPSRC under EP/C5228771 and EP/E054129/1 and at Cornell by the NSF under DMR-0457533,-0806629.

References

1. V. Ambegaokar, P.G. deGennes, D. Rainer, Phys. Rev. A **9**(6), 2676 (1974)
2. T. Fujita, M. Nakahara, T. Ohmi, T. Tsuneto, Prog. Theor. Phys. **64**(2), 396 (1980)
3. Y.H. Li, T.L. Ho, Phys. Rev. B **38**(4), 2362 (1988)
4. A.L. Fetter, S. Ullah, J. Low Temp. Phys. **70**(5/6), 515 (1989)
5. Y. Nagato, K. Nagai, Physica B **284–288**(1), 269 (2000)
6. A.B. Vorontsov, J.A. Sauls, Phys. Rev. Lett. **98**(4), 045301 (2007)
7. M.R. Freeman, R.C. Richardson, Phys. Rev. B **41**(16), 11011 (1990)
8. K. Kawasaki, et al., Phys. Rev. Lett. **93**(10), 105301 (2004)
9. T. Kawae, et al., J. Low Temp. Phys. **111**(5/6), 917 (1998)
10. Hoya Corporation, Optics Division, 3400, Edison Way, Fremont, CA 94538
11. L.V. Levitin, et al., Appl. Phys. Lett. **91**(26) (2007)
12. S. Takagi, J. Phys. C **8**, 1507 (1975)
13. L.H. Kjaldman, J. Kurkijärvi, D. Rainer, J. Low Temp. Phys. **33**(5/6), 577 (1978)
14. L.V. Levitin, et al., J. Low Temp. Phys. This issue
15. D.S. Greywall, Phys. Rev. B **33**(11), 7520 (1986)
16. D. Einzel, J. Low Temp. Phys. **54**(5/6), 427 (1984)